Molecular structure and nitrite-bonded study on copper(II) complexes of N,N-dialkyl,N′-benzyl-ethylenediamine; Synthesis, spectroscopic characterization, X-ray structure, steric ef...

ARTICLE *in* POLYHEDRON · APRIL 2015

Impact Factor: 2.01 · DOI: 10.1016/j.poly.2015.01.044

5 AUTHORS, INCLUDING:

Hamid Golchoubian

University of Mazandaran

79 PUBLICATIONS **524** CITATIONS

SEE PROFILE

Ehsan Rezaee

University of Mazandaran

15 PUBLICATIONS **80** CITATIONS

SEE PROFILE

Golasa Moayyedi

University of Mazandaran

8 PUBLICATIONS **34** CITATIONS

SEE PROFILE

Davood Farmanzadeh

University of Mazandaran

29 PUBLICATIONS **116** CITATIONS

SEE PROFILE

Polyhedron 90 (2015) 108–117

Contents lists available at ScienceDirect

Polyhedron

journal homepage: www.elsevier.com/locate/poly

Molecular structure and nitrite-bonded study on copper(II) complexes of *N*,*N*-dialkyl,*N*′-benzyl-ethylenediamine; synthesis, spectroscopic characterization, X-ray structure, steric effect and density functional theory calculations

Hamid Golchoubian *, Zeynab Khazaee, Ehsan Rezaee, Golasa Moayyedi, Davood Farmanzadeh

Department of Chemistry, University of Mazandaran, Babolsar 47416-95447, Iran

ARTICLE INFO

Article history:
Received 21 December 2014
Accepted 29 January 2015
Available online 14 February 2015

Keywords:
Copper(II)
DFT study
Linkage isomer
X-ray structure
Nitro

ABSTRACT

Presented here is an investigation on the geometric (molecular) structures, spectroscopic properties and electronic structures of copper(II)-nitrite complexes as a function of steric effects, utilizing a set of closely related co-ligands. The prepared complexes, with the general formula $[CuL^{R}(\eta^2\text{-}ONO)_2]$ where L^{R} is *N*,*N*-dialkyl,*N*′-benzyl-ethylenediamine and R is methyl, ethyl or isopropyl moieties, were structurally characterized by physico-chemical and spectroscopic methods. An X-ray diffraction study on $CuL^{Me}(\eta^2\text{-}ONO)_2]$ and $CuL^{Et}(\eta^2\text{-}ONO)_2]$ reveals that the copper(II) center in both compounds is located in a distorted octahedral environment through coordination of two amine nitrogen atoms and four oxygen atoms of the nitrite ligands. Depending on the steric crowding of the co-ligand, the coordination mode is either symmetric or asymmetric bidentate, as is evident from X-ray crystallography and IR spectroscopy. The relative stability of linkage isomers of these compounds, along with a *tert*-butyl derivative complex, was investigated using density functional theory (DFT) calculations. The calculated results demonstrated that in all cases the bidentate η^2-ONO isomer is more stable than the four-coordinated nitro isomer ($\eta^1\text{-}NO_2$). However, the differences in the relative stability decrease as the steric hindrance in the co-ligand increases. The vibrational spectra of the complexes were assigned using DFT calculations. In support with the X-ray structure, the results reveal that ν_{as}(N–O) splits into two bands, with the separation increasing from $[CuL^{Me}(\eta^2\text{-}ONO)_2]$ through to $[CuL^{tert\text{-}buty}(\eta^2\text{-}ONO)_2]$. That is at least partially dictated by steric factors within the molecules, imposed by the alkyl groups of the co-ligand. The UV–Vis absorption spectra are presented and analyzed with the help of time-dependent density functional theory (TD-DFT) calculations.

1. Introduction

The nitrite ion, NO_2^-, behaves as an ambidentate ligand that may coordinate through oxygen and/or nitrogen atoms (Scheme 1). When it is coordinated through the nitrogen atom, the resulting M–NO_2 species is termed a "nitro" complex, and when it is coordinated through a single oxygen atom, the M–ONO species is termed a "nitrito" complex. Alternatively the nitrite can be coordinated via both oxygen atoms in a bidentate approach. These flexible coordination modes of the nitrite ion result in special attention from chemists [1–4]. Basically, the relative stability of the linkage isomers is correlated with the sigma-donating affinities of the two donor atoms of the ambidentate ligand, so that the stable isomer is formed with the stronger donor atom. The softness or hardness of the metal ions is another parameter controlling the coordination mode of the NO_2^- ion [5]. Furthermore, steric crowding functions as a crucial role, as both binding modes involve different steric hindrances toward the ancillary ligand present in the coordination sphere [6,7].

There is significant current attention in nitrite complexes of copper(II) owing to the nitrite-reductase functions of copper containing enzymes. [8] These enzymes are part of the biological denitrification process [9–11]. It was also shown that in the active site of the enzyme the nitrite group is coordinated to the copper center in the η^2-ONO mode [12–15]. The nitrite adducts of the copper containing nitrite reductases catalyze the reduction of nitrite to nitric oxide (NO), which is a key step in denitrification [16–18]. Tolman used a copper complex containing a chelating

* Corresponding author. Tel./fax: +98 1125342350.
E-mail address: h.golchobian@umz.ac.ir (H. Golchoubian).

http://dx.doi.org/10.1016/j.poly.2015.01.044
0277-5387/

NO_2^- group with η^2ONO donors as a nitrite reductase model complex [19].

In terms of hard and soft acid/base, the copper(II) ion is a borderline Lewis acid and it is expected to bind through the O, N and O,O donors of the NO_2^- ligand. Another aspect of copper(II) complexes is the coordination geometry around the metal ion, which can exist as coordination numbers four and six. In six-coordinate complexes, the copper(II) ion usually demonstrates an octahedral or distorted octahedral structure, while the square planar geometry is the typical structure of the coordination number four. The difference in geometry is sometimes dependent on the nature of other groups coordinated to the metals as a result of either steric or electronic factors.

Computational studies have been accompanied by experimental analysis to get further insight into the different stabilities of NO_2^- linkage isomers. Di-nitrite copper(II) complexes containing an ancillary bidentate ligand are suitable models to have a computational assessment between coordination number four, with nitro–copper(II) bonds and a square planar structure, and six, with the η^2-ONO coordination mode and an octahedron geometry, as a result of steric crowding imposed by the ancillary ligand. Density functional theory (DFT) is a computational quantum mechanical modelling method used to investigate many-body systems. Recently, DFT methods have become very popular in order to understand detailed electronic structures of complicated coordination compounds and also to predict linkage isomerism of various systems [20,21]. Several DFT studies on the linkage isomerism of complexes containing a nitrite ligand have previously been performed [7,22–24].

In this work, dinitrite copper(II) complexes with *N*,*N*-dialkyl,*N*′-benzyl-ethylenediamine (L^R), $[CuL^R(NO_2)_2]$, using different alkyl groups were prepared experimentally or computationally to investigate the effect of (i) the steric crowding around the copper center on the coordination mode of the nitrite group, (ii) the coordination number of the nitrite and (iii) the effect of the nature of the alkyl substituents on the structures and spectroscopic properties of the Cu(II)-nitrite complexes. Crystal structures for the complexes $[CuL^{Me}(\eta^2\text{-ONO})_2]$ and $[CuL^{Et}(\eta^2\text{-ONO})_2]$ are presented. The electronic structures of the compounds were investigated using vibrational (IR) and electronic (UV–Vis) absorption spectroscopy techniques coupled with DFT calculations. Based on our knowledge, such an investigation has not been reported for copper(II) complexes before.

2. Experimental

N,*N*-dimethyl,*N*′-benzyl-ethylenediamine and *N*,*N*-diethyl,*N*′-benzyl-ethylenediamine were prepared according to our published procedure [25]. All solvents were spectral grade and all other reagents were used as received. All the samples were dried to a constant weight under a high vacuum prior to analysis. Conductance measurements were made at 25 °C with a Jenway 400 conductance meter on 1.00×10^{-3} M samples in selected solvents. Infrared spectra measurements were carried out using KBr disks on a Bruker FT-IR instrument. The electronic absorption spectra were measured using a Braic2100 model UV–Vis spectrophotometer. Elemental analyses were performed on a LECO 600 CHN elemental analyzer. Absolute metal percentages were determined by a Varian-spectra A-30/40 atomic absorption-flame spectrometer.

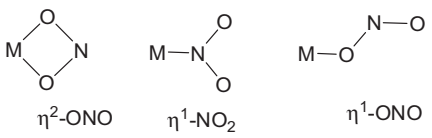

Scheme 1. Different binding modes of nitrite in mononuclear complex.

2.1. Synthesis

2.1.1. Preparation of *N*,*N*-diisopropyl,*N*′-benzyl-ethylenediamine, L^{iso}

The same procedure as for $L^{Me,Et}$ was used for the preparation of the ligand L^{iso}, using 2-(diisopropylamino)ethylamine instead of *N*,*N*-dimethyl (or diethyl)-ethylenediamine. The product was obtained as a yellow oil in a yield of 65%. Selected IR data (ν/cm^{-1}): 3419 (br. m, N–H str.), 2970 (s, C–H str. aliphatic), 2877 (w, N–CH– str.), 1550 (s, C–N str.), 1393 (m, N–H bend.). ^{1}H NMR (400 MHz in $CDCl_3$), δ (ppm): 1.01 (d, J = 6.4 Hz, 6H, $(CH_3)_2$CH–), 2.70 (t,d, J = 5.2 Hz, J = 1.2 Hz, 2H,–CH_2–CH_2–N), 2.77 (t, 2H, J = 5.2 Hz, $((CH_3)_2CH)_2NCH_2CH_2NH$–), 2.95 (heptet, 1H, $(CH_3)_2CH$–)), 3.35 (s, br, H, –NH–), 3.94 (s, 2H, –NH–CH_2–Ph), 7.28–7.39 (m, 5H, $-C_6H_5$). ^{13}C NMR (100 MHz in $CDCl_3$), δ (ppm): 20.50 ($(CH_3)_2$-CH–), 42.58 ($((CH_3)_2CH)_2NCH_2CH_2NH$–), 45.44 (–$NCH_2CH_2NH$–), 48.07 (Ph–$CH_2NH$–), 52.02 ($(CH_3)_2CH$–), 127.85, 128.74, 136.81 and 176.79 ($-C_6H_5$).

2.1.2. Preparation of $[Cu(L^{Me})(\eta^2\text{-ONO})_2]$, **1**

To a solution of *N*,*N*-dimethyl,*N*′-benzyl-ethylenediamine (1 mmol, 0.178 g) in ethanol (5 ml) was slowly added $Cu(OAc)_2 \cdot H_2O$ (1 mmol, 0.199 g) in ethanol (20 ml). The resultant mixture was stirred for 30 min at room temperature. A solution of $NaNO_2$ (2 mmol, 0.138 g) in water (15 ml) was then added, whereupon the initial blue color changed to green. After overnight stirring at room temperature, the desired compound precipitated. The green solid was collected by filtration, washed with water and dried in vacuo. The crude compound was recrystallized from diffusion of diethyl ether into an acetonitrile solution. A typical yield was 60%. Selected IR data (ν/cm^{-1} KBr disk): 3181 (m, N–H str.), 1463 (m, CH_2–Ph str.), 1350 (s, NO_2^- str.), 1170, 1167 (s, NO_2^- str.), 849 (w, NO_2^- str.). *Anal.* Calc. for $C_{11}H_{18}CuN_4O_4$ (MW = 333.83 g mol^{-1}): C, 39.58; H, 5.43; N, 16.78; Cu, 19.04. Found: C, 39.46; H, 5.37; N, 16.49; Cu, 19.12%. Molar conductance (Λ_m/Ω^{-1} cm^2 mol^{-1}): in NM, 6; in NB, 5; in ACN, 8; in AC, 15; in EtOH, 10; in MeOH, 10; in DMF, 12.

2.1.3. Preparation of $[Cu(L^{Et})(\eta^2\text{-ONO})_2]$, **2**

This complex was prepared by a method similar to that used for $[Cu(L^{Me})(\eta^2\text{-ONO})_2]$, except that L^{Et} was used in place of L^{Me}. The compound was obtained as a green solid in a typical yield of 90%. Selected IR data (ν/cm^{-1} using KBr): 3232 (m, N–H str.), 1456 (m, CH_2–Ph str.), 1347 (s, NO_2^- str.), 1197, 1171 (s, NO_2^- str.), 844 (w, NO_2^- str.). *Anal.* Calc. for $C_{13}H_{22}CuN_4O_4$ (MW = 361.89 g. mol^{-1}): C, 43.15; H, 6.13; N, 15.48; Cu, 17.56. Found: C, 43.19; H, 6.15; N, 15.36; Cu, 17.44%. Molar conductance (Λ_m/Ω^{-1} cm^2 mol^{-1}): in NM, 4; in NB, 1; in ACN, 9; in AC, 8 in EtOH, 12; in MeOH, 28, in DMF, 8.

2.1.4. Preparation of $[Cu(L^{iso})(\eta^2\text{-ONO})_2]$, **3**

This complex was prepared by a method similar to that used for $[Cu(L^{Me})(\eta^2\text{-ONO})_2]$, except that L^{iso} was used in place of L^{Me}. The compound was obtained as a green solid in a typical yield of 30%. Selected IR data (ν/cm^{-1} using KBr): 3154 (m, N–H str.), 1460 (m, CH_2–Ph str.), 1393 (s, NO_2^- str.), 1271, 1217 (s, NO_2^- str.), 830 (w, NO_2^- str.). *Anal.* Calc. for $C_{15}H_{26}CuN_4O_4$ (MW = 389.94 g mol^{-1}): C, 46.20; H, 6.72; N, 14.37; Cu, 16.30. Found: C, 46.04; H, 6.66; N, 14.28; Cu, 16.41%. Molar conductance (Λ_m/Ω^{-1} cm^2 mol^{-1}): in NM, 3; in NB, 7; in ACN, 9; in AC, 1; in EtOH, 9; in MeOH, 22; in DMF, 3.

2.2. X-ray crystallographic study

The X-ray data for compounds **1** and **2** were collected on a Bruker–Nonius X8 ApexII diffractometer equipped with a CCD area detector using graphite-monochromated Mo Kα radiation (λ = 0.71073 Å) generated from a sealed tube source. Data were collected and reduced by SMART and SAINT software [26] in the Bruker package. The structures were solved by direct methods [27] and then developed by least squares refinement on F^2 [28,29]. The non-H atoms found in the electron density map were refined anisotropically. All H atoms were placed in calculated positions with the 'riding-model technique'. Compound **2** was found to be disordered and the ethyl groups and $-CH_2-CH_2-$ moiety of the diamine ligand were refined in two positions with population parameters of 0.5 and 0.5. Details concerning collection and analysis are reported in Table 1.

2.3. Computational method

All calculations were completed with the GAUSSIAN 09 program [30] and the output files were pictured by the GAUSS VIEW 05 software program [31]. Harmonic vibrational frequency analyses were made to characterize the optimized geometries as potential minima on the potential energy surface. The spin-unrestricted Kohn–Sham method was employed for the Cu(II)(η^2-ONO), Cu(II)(η^1-ONO) and Cu(II)(η^1–NO_2) coordination modes of nitrite by assuming the doublet spin states. We used four different exchange–correlation functionals, mPWPW91GEN (using the Perdew–Wang exchange as modified by Adamo and Barone combined with the PW91 correlation) [32], B3PW91 GEN (the non-local correlation provided by Perdew/Wang) [33], B3LYP GEN (Becke's three parameter hybrid model using the Lee–Yang Parr correlation functional in the GEN mode) [34,35] and B3LYP 6-31G+ methods with the 6-31G$^+$ (*d*,*p*) basis set [36] for C, H, N and O atoms, and the LANL2DZ pseudo-potential for the Cu^{2+} atom [37]. The B3PW91 and B3LYP functionals were selected since these functionals have been utilized most extensively in DFT calculations of coordination compounds [38]. The mPWPW91 functional was employed since Ghosh et al. has previously demonstrated that this functional works well for the consideration of electronic structures as well as for the assignment of experimentally achieved absorption spectra [39]. The X-ray crystallographic structure of [CuL^{Me}(η^2-ONO)$_2$] and [CuL^{Et}(η^2-ONO)$_2$] were used to generate the initial complex geometries and to calibrate the method. The optimized geometries of the structural isomers were tested by performing a frequency calculation at the DFT levels. The lack of imaginary frequency proves the reality of the calculated vibrational spectra, thus they correspond to true energy minimum [40]. After finding the geometry-optimized structure of the stable isomer of each complex, optimization in solvent was then performed. The solvent effect was simulated using the polarizable continuum model with the integral equation formalism (CPCM). The electronic structures of the calculated molecules were analyzed utilizing the natural bond orbital (NBO) method and the associated natural population analysis (NPA) [41]. It should be mentioned that the NBO method is particularly valuable for inorganic complexes, because the approach provides a good description of the charge distribution which is less sensitive to computational parameters such as basis sets [42]. The electronic spectra of the compounds were calculated with the TD-DFT method.

Table 1
Crystal data and structure refinement for complexes **1** and **2**.

Complex	[Cu(L^{Me})(η^2-ONO)$_2$]	[Cu(L^{Et})(η^2-ONO)$_2$]
Empirical formula	$C_{11}H_{18}CuN_4O_4$·	$C_{13}H_{21}CuN_4O_4$
Formula weight	333.84	361.88
Color	needle, green	needle, green
Temperature (K)	296(2)	293(2)
Wavelength (Å)	0.71073	0.71073
Crystal system	orthorhombic	triclinic
Space group	$P2_12_12_1$	$P\bar{1}$
Crystal size (mm)	0.3 × 0.1 × 0.1	0.2 × 0.2 × 0.1
Unit cell dimensions		
a (Å)	10.7400(4)	7.8402(3)
b (Å)	11.2567(4)	10.2102(5)
c (Å)	12.4998(4)	11.5840(5)
α (°)	90	69.8296(190
β (°)	90	84.082(2)
γ (°)	90	75.202(2)
V (Å^3)	1511.19(9)	841.44(6)
Z	2	2
Calculated density (Mg/m^3)	1.397	1.428
μ(mm^{-1})	1.458	1.320
F (000)	664	378
θ range for data collection (°)	2.50–27.99	2.36–33.03
Index ranges	$-14 \leqslant h \leqslant 14$ $-14 \leqslant k \leqslant 14$ $-16 \leqslant l \leqslant 16$	$-12 \leqslant h \leqslant 12$ $-15 \leqslant k \leqslant 15$ $-17 \leqslant l \leqslant 17$
Reflections collected/unique	58414/3641 [R(int) = 0.0767]	44410/6237 [R(int) = 0.0187]
Completeness to θ = 27.99	100%	98.2%
Absorption correction	semi-empirical from equivalents	semi-empirical from equivalents
Refinement method	full-matrix least-square on F^2[a]	full-matrix least-square on F^2[a]
Data/restraints/parameters	4489/0/185	6237/0/261
R indices[a] [2806 with $I > 2\sigma(I)$][b]	R_1 = 0.0436, wR_2 = 0.0816	R_1 = 0.0249, wR_2 = 0.0708
Goodness-of-fit on F^2[c]	0.936	1.035
R indices (all data)	R_1 = 0.0796, wR_2 = 0.0961	R_1 = 0.0306, wR_2 = 0.0743
Largest difference in peak and hole, e Å^{-3}	0.253 and −0.321	0.244 and −0.403

[a] $R = \Sigma(||F_o| - |F_c||)/|\Sigma|F_o|$.
[b] $wR = \{[(\Sigma[F_o^2 - F_c^2)^2]/\Sigma w[(F_o^2)^2]\}^{1/2}$.
[c] $S = \Sigma[w(F_o^2 - F_c^2)^2/(N_{obs} - N_{param})$.

3. Results and discussion

3.1. Synthesis

A straightforward reaction between the bidentate ligand L (L^{Me}, L^{Et} or L^{iso}), copper(II) acetate monohydrate and $NaNO_2$ in ethanol affords a green crystalline solid. Microanalytical, IR and solution electrical conductivity data suggest that in all cases the complexes have the composition [Cu(L)(η^2-ONO)$_2$]. This was finally confirmed by X-ray structural analysis. It is worth mentioning here that the motivation for investigating the binding of the nitrite ion was to investigate the effect of the steric constraints arising from alkyl groups attached to the ethylenediamine group on the denticity of the nitrite groups. The molar conductivity values of the complexes in various organic solvents demonstrate the non-electrolytic nature of the complexes.

3.2. X-ray structure

The structures of complexes **1** and **2** are depicted in Figs. 1 and 2, while the main bond distances and angles are given in Tables 2 and 3. The crystal structures of the complexes have a number of interesting common features and at the same time there are some differences. Both structures consist of a neutral [CuL(η^2-ONO)$_2$] unit, in which the copper atoms are surrounded by nitrogen atoms of the ethylenediamine derivative from the L$^{Me/Et}$ ligand and four oxygen atoms from two nitrito (η^2ONO) ligands. The local molecular structure of the copper(II) ion involves a tetrahedrally distorted

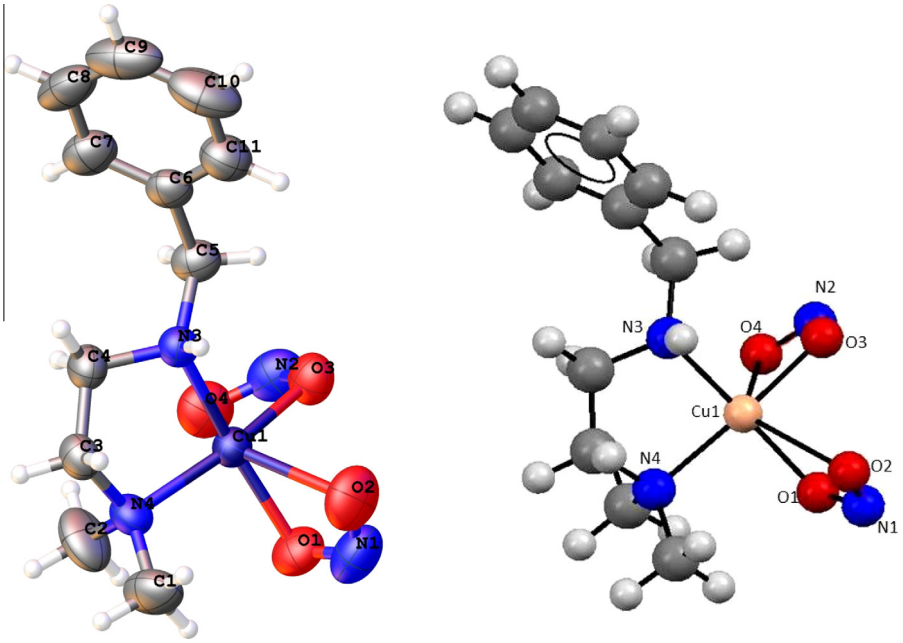

Fig. 1. ORTEP view (right) and the optimized geometry (left) of complex **1** together with its labelling.

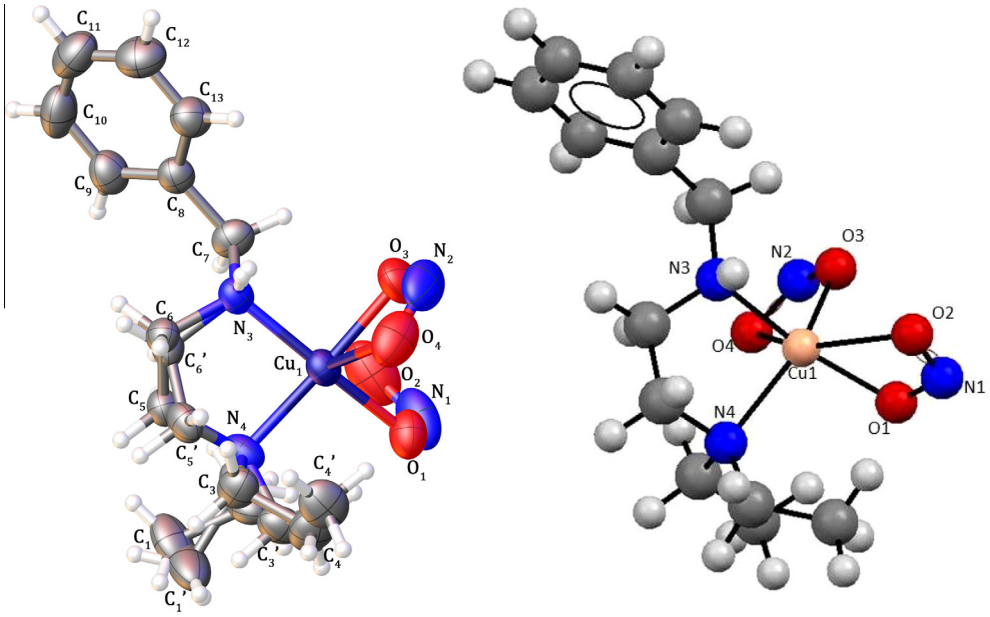

Fig. 2. ORTEP view (right) and the optimized geometry (left) of complex **2** together with its labelling.

elongated octahedral $CuN_2O_2O'_2$ chromophore, where the N(3) and N(4) atoms from the diamine along with the O(1) and O(3) atoms of the nitrites are located in the plane, and other two oxygen atoms [O(2) and O(4)] of the nitrites occupy apical positions. Two oxygen atoms from each nitrite group bond in-the-plane with Cu–O distances of 1.992(2) and 2.011(2) Å in **1** and 1.9874(10) and 2.0260(10) Å in **2**, along with two nitrogen atoms of the ligand L, forming a markedly tetrahedral distorted square base with a dihedral angle of 22.52(11) and 11.85(2)° in compound **1** and **2**, respectively, where the N–Cu–N and O–Cu–O planes cross. The four basal donor atoms, N(3), N(4), O(1) and O(3), in compound **1** deviate out from their least squares plane by −0.268(1), 0.276(1), −/0.270(1) and 0.263(1) Å, respectively, whereas, the deviations in compound **2** for the N(4), N(3), O(1) and O(3) basal donor atoms are 0.140(1), −0.145(1), /0.136(1) and −0.263(1) Å, respectively. In both complexes the Cu atoms are located in the plane. The second oxygen atom from each nitrite group is bent towards the Cu atom to complete the fifth, O(2), and sixth, O(4), coordination sites in approximately axial positions at longer distances of 2.370(3) and 2.458(2) Å in compound **1** and 2.4561(11) and 2.4313(10) Å in **2**, respectively. Furthermore, the axial ligands show the greatest distortion from the idealized octahedron geometry. The O(2)–Cu–O(4) angle, 134.82(3)° in **1** and 127.47(13)° in **2**, is substantially smaller than the ideal value of 180°. This is at least partially dictated by steric factors within the molecule imposed by the alkyl groups. The nitrite ions display their expected geometry, with the longer

Table 2
Selected bond lengths (Å) and angles (°) for complex **1**.

Bond distances (Å)			
Cu–N(3)	2.010(2)	Cu–O(4)	2.458(4)
Cu–N(4)	2.019(2)	O(1)–N(2)	1.259(4)
Cu–O(1)	1.992(2)	O(3)–N(1)	1.267(4)
Cu–O(3)	2.011(2)	N(1)–O(4)	1.226(4)
Cu–O(2)	2.370(3)	O(2)–N(2)	1.209(4)
Bond angles (°)			
O(1)–Cu–N(3)	166.13(10)	O(3)–Cu–N(4)	162.77(11)
O(1)–Cu–O(3)	88.75(10)	O(1)–Cu–O(2)	55.70(10)
N(3)–Cu–O(3)	96.13(9)	N(3)–Cu–O(2)	111.23(10)
O(1)–Cu–N(4)	93.17(10)	O(3)–Cu–O(2)	89.33(10)
N(3)–Cu–N(4)	86.01(9)	N(4)–Cu–O(2)	105.88(11)
O(2)–Cu–O(4)	134.81(13)	N(3)–Cu–O(4)	100.32(13)
O(3)–Cu–O(4)	54.73(10)	N(4)–Cu–O(4)	108.02(13)
O(2)–N(1)–O(1)	113.6(3)	O(4)–N(2)–O(3)	114.2(3)

Table 3
Selected bond lengths (Å) and angles (°) for complex **2**.

Bond distances (Å)			
Cu–N(3)	2.0032(10)	Cu–O(4)	2.4313(10)
Cu–N(4)	2.0448(9)	O(1)–N(1)	1.2620(18)
Cu–O(1)	2.0261(10)	O(3)–N(2)	1.258(2)
Cu–O(3)	1.9874(10)	N(2)–O(4)	1.234(2)
Cu–O(2)	2.4561(11)	O(2)–N(1)	1.222(2)
Bond angles (°)			
O(1)–Cu–N(3)	170.11(4)	O(3)–Cu–N(4)	172.54(4)
O(1)–Cu–O(3)	89.52(5)	O(1)–Cu–O(2)	54.61(5)
N(3)–Cu–O(3)	90.40(4)	N(3)–Cu–O(2)	115.56(4)
O(1)–Cu–N(4)	95.00(4)	O(3)–Cu–O(2)	84.37(4)
N(3)–Cu–N(4)	86.16(4)	N(4)–Cu–O(2)	127.47(5)
O(2)–Cu–O(4)	127.50(3)	N(3)–Cu–O(4)	97.86(4)
O(3)–Cu–O(4)	54.66(5)	N(4)–Cu–O(4)	119.26(5)
O(2)–N(1)–O(1)	113.76(14)	O(4)–N(2)–O(3)	112.95(12)

Table 4
Hydrogen bonds for complexes **1** and **2** (D, donor atom; A, acceptor atom).

D-H···A	d(D-H) Å	d(H···A) Å	d(D···A) Å	D-H···A (°)
Complex **1**				
N(3)-H(3)···O(4)#1[a]	0.91	2.20	3.088(3)	165.9
Complex **2**				
N(3)-H(3)...O(2)#1 [b]	0.91	2.15	3.0209(15)	160.7

[a] Symmetry transformations used to generate equivalent atoms: #1 $-x+1, y-1/2, -z+1/2$.
[b] Symmetry transformations used to generate equivalent atoms: #1 $-x, -y, -z+2$.

N–O bonds involved in coordination [O(1)–N(1) = 1.259(4) Å in **1** and 1.2620(18) Å in **2** and O(3)–N(2) = 1.267(4) Å in compound **1** and 1.258(2) Å in compound **2**] with regard to the weakly coordinated N–O bonds [N(1)–O(2) = 1.209(4) Å in **1** and 1.224(2) Å in **2** and N(2)–O(4) = 1.226(4) Å in **1**, and 1.234(2) Å in **2**]. Nevertheless, the differences are less than that found in a purely monodentate nitrite ligand (1.290 and 1.207 Å) [43]. In addition, The angles at the nitrogen atoms of the nitrite groups [113.6(3)° and 114.2(2)° in compound **1** and 112.95(12)° and 113.76(14)° in compound **2**] are between that found in the purely monodentate nitrito-coordination (115.0°) [44] and the bidentate nitrito-coordination (111°–112°) [44,45]. Therefore, the coordination mode of the weakly coordinated oxygen atoms to the copper ion in both complexes is intermediate between purely monodentate nitrito-coordination (η^1-ONO) and bidentate nitrito-coordination (η^2-ONO) [43]. The planes of the dinitrite groups in each complex are almost perpendicular to each other [83.4(3)° for **1** and 86.4(2)° for **2**]. In spite of similar environments about the copper atom for both complexes, the local molecular geometries around the copper(II) ions are not similar, with a slightly more elongated axial positions for **2** [Cu-O(2) = 2.456(2) Å] as compared to **1** [Cu–O(2) = 2.370(3) Å]. These differences in the nitrite binding geometry can be viewed as a direct reflection of the divergent steric influences of the alkyl substitution in the coligand. Both complexes have significant differences in the tetrahedral twist of the basal plane [38.6(1)° in **1** and 21.2(2)° in **2**], the O(2)–Cu–O(4) angle [134.7(3)° in **1** and 127.47(2)° in **2**], one of the ethyl groups [C(3) and C(4)] and the carbon atoms of chelate ring. The N–H bonds of the secondary amine groups of both complexes **1** and **2** are involved in intermolecular hydrogen bonds. Details about the hydrogen bonding are shown in Table 4. In the crystal lattice of compound **1**, N(3)–H(3)···O(4) hydrogen bonds [2.20(2) Å] link neighbouring molecules in a zig-zag fashion along the "*b*" axis (Fig 3). However, in compound **2**, an N(3)–H(3)···O(4) hydrogen bond links the compound into a dimer, which is translated one unit cell along the '*c*' direction (Fig. 4).

3.3. Theoretical consideration

To obtain insight into the geometric and electronic properties of the complexes, DFT calculations were performed on the complexes with a crowded version of the coligand L^R, where more bulky substituents were added. In order to provide a systematic comparison, geometry optimizations were performed on the structures containing the conceivable coordination modes of nitrite to a mononuclear copper center, namely bidentate Cu-(η^2-ONO), monodentate Cu-(η^1-ONO) (nitrito) and monodentate Cu-(η^1-NO_2) (nitro) complexes (Scheme 2). First, we started by optimizing the geometry of the complexes [Cu(L^{Me})(η^2-ONO)$_2$] and [Cu(L^{Et})(η^2-ONO)$_2$] in the gas phase with different levels of calculations in order to calibrate the method. The optimized geometries are shown in Figs 1 and 2 (along with ORTEP views of the complexes) and the experimental and calculated bond lengths and bond angles are shown in Tables S1 and S2 in the Supplementary information. Although the agreement with those distances and angles experimentally determined are very good, B3LYP(6-31G+) provides the least deviation among all levels of calculations used. The deviation between theory and experiment for the metal–ligand bond distances is only of the order of 1 pm. Moreover, this was supported by a comparison of the calculated and experimental vibrational frequencies of complexes, as shown in Fig. 5 and Fig. S1 in the Supplementary information. Next, the B3LYP level calculations were applied to Cu-(η^1-NO_2), Cu-(η^1-ONO) and Cu-(η^2-ONO) coordination modes of all twelve complexes shown in Scheme 2. In all cases the N-bound species (η^1-NO_2) is predicted to be higher in energy, while the monodentate O-bound species (η^1-ONO) is isoenergetic with the bidentate O-bonded (η^2-ONO) species where the second oxygen coordinates to a copper center. As a result, the feasible coordination modes of the nitrite in the mononuclear copper(II) complexes were Cu-(η^1-NO_2) and Cu-(η^2-ONO) (see Fig S2 and S3 in the Supplementary information). The relative energies of the two coordination modes for the Cu(II) species are gathered in Table S3 in the Supplementary information. The obtained results show that the bidentate, Cu-(η^2-ONO) coordination mode is the preferred one in all cases (cf. Table S3 in the Supplementary information). However, a closer inspection of the data shows that as the steric hindrance around the copper(II) increases, the difference in the relative energy of the bidentate, Cu-(η^2-ONO) coordination and Cu-(η^1-NO_2) coordination ($\Delta E = E^{O,O} - E^{N}$) deceases.

As discussed in the X-ray crystallography section, one of the Cu–O bonds of the nitrite groups [Cu–O(2)] is sensitive to steric crowding around the copper center. This phenomenon was investigated in Cu(L^R)(η^2-ONO)$_2$ complexes with different alkyl groups (R). In this regard, the Cu–O bond distances of the nitrite groups,

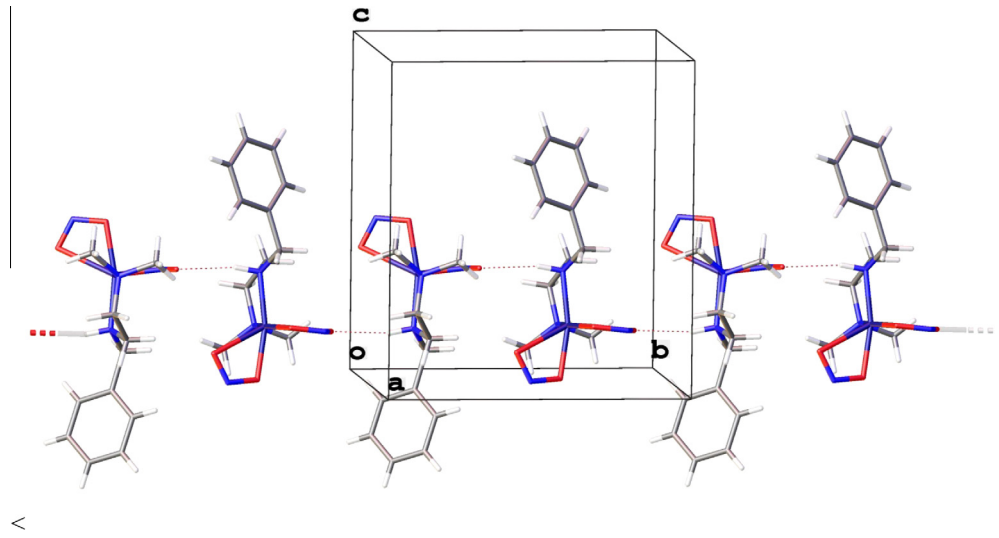

Fig. 3. One-dimensional zig-zag-like chain structure of compound **1** along the *b*-axis with hydrogen bonds indicated by dotted lines.

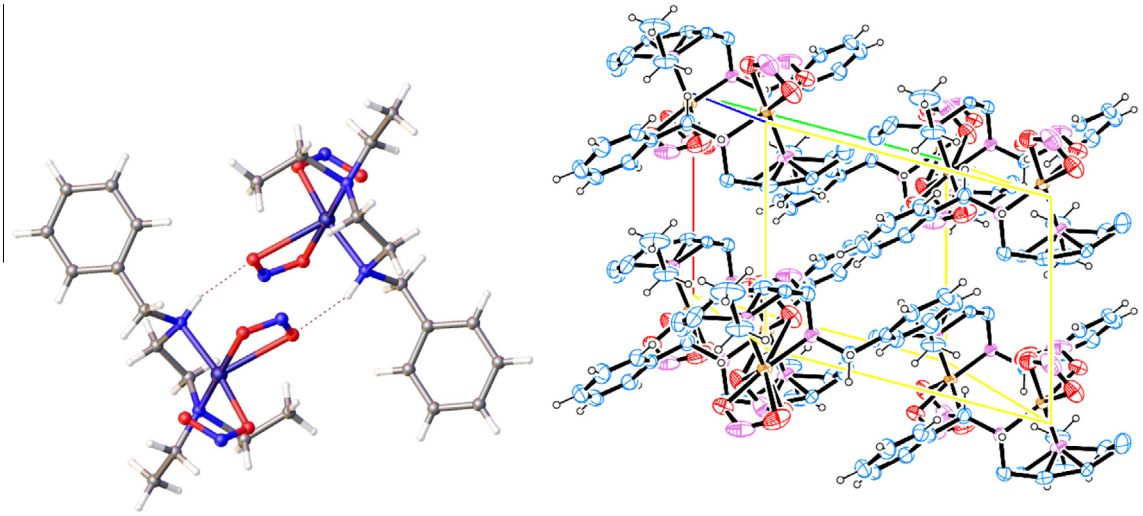

Fig. 4. The intermolecular hydrogen bonding in the dimeric structure (top) and crystal packing of complex **2** along the '*c*' axis (bottom).

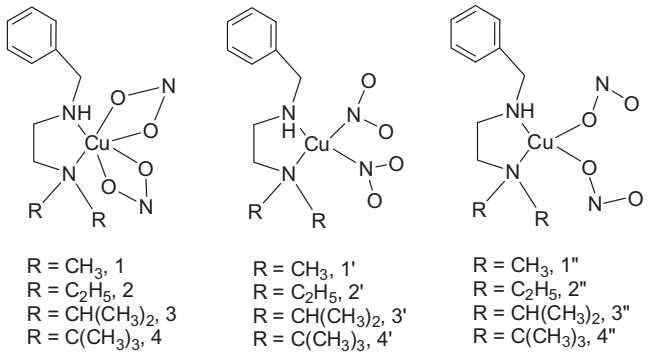

Scheme 2. Possible coordination mode of the nitrite as bidentate-(η^2-ONO) (left), monodentate-(η^1-NO_2), (middle) and monodentate-(η^1-ONO) (right).

which were determined computationally by the DFT method at the B3LYP(6-31G+) level, were examined (see Tables S1, S2, S4 and S5 in the Supplementary information). In all the cases one of the nitrite ligands (O(3)N(2)O(4)) demonstrates a minor variation in the Cu–O bond length from methyl through to *tert*-butyl substitution (ΔCu–O(4) = 0.106 Å and ΔCu–O(3) = 0.050 Å). In the second nitrite group (O(1)N(1)O(2)), the variation in the Cu–O(1) bond distance, where the ligand resides in the base, is trivial (ΔCu–O(1) = 0.046 Å), but the differences in Cu–O(2), located in the axial position, is significant (ΔCu–O(2) = 0.188 Å). The Cu–O(2) bond distance increases as the alkyl group becomes larger (2.456 Å in $[Cu(L^{Me})(\eta^2\text{-ONO})_2]$, 2.532 Å in $[Cu(L^{Et})(\eta^2\text{-ONO})_2]$, 2.587 Å in $[Cu(L^{iso})(\eta^2\text{-ONO})_2]$ and 2.709 Å in $[Cu(L^{t\text{-but}})(\eta^2\text{-ONO})_2]$,). These results show that the increase in the steric hindrance facilitates a square pyramidal environment in the copper complex.

3.3.1. Vibrational analysis

In the IR spectra, there is a sharp band at 3176 cm^{-1} for compound **1**, 3192 cm^{-1} for compound **2** and 3154 cm^{-1} for compound **3**, which are characteristic of a secondary amine group. As it was pointed out before, in monomeric metal ion complexes, the nitrite ion can coordinate through oxygen and/or nitrogen atoms in η^2-ONO, η^1-NO_2 (nitro) and η^1-ONO (nitrito) modes. The criteria for

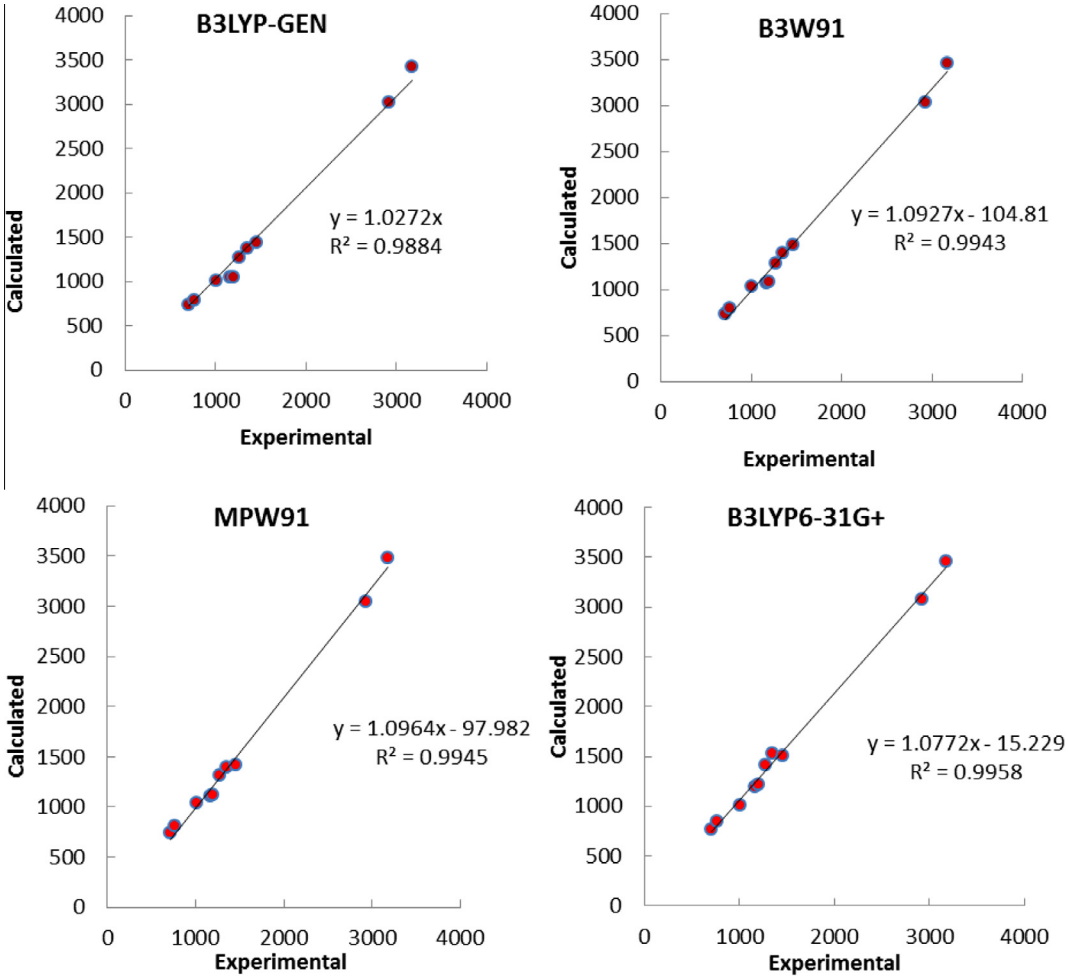

Fig. 5. Relationship between the calculated and the observed vibrational frequency values for complex **1**.

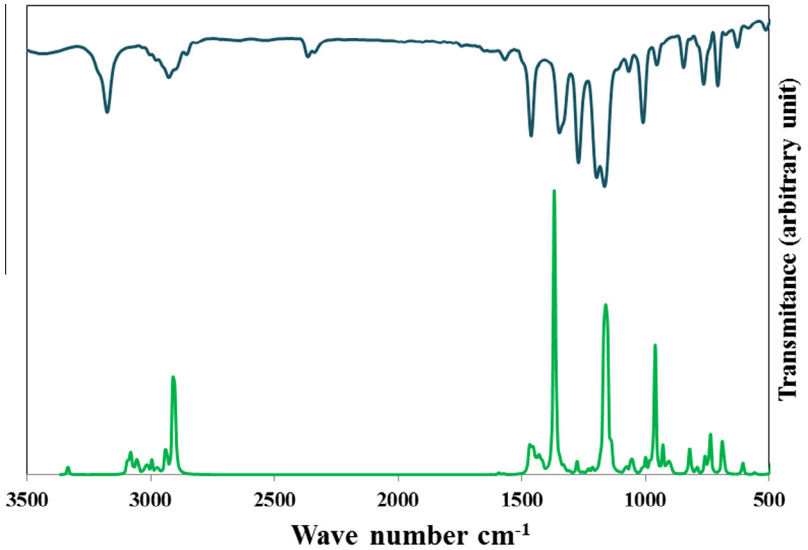

Fig. 6. Experimental (top) and calculated IR spectra of complex **1**.

establishing the bonding mode in complexes have been investigated based on the frequency ranges of these species, that is the frequencies of the O–N bond. It has been known that for nitrito complexes, the two NO stretching frequencies ν(N=O) and ν(N–O) are well separated, falling in the ranges 1510–1400 and 1100–900 cm^{-1}, respectively. The separation is much smaller for the nitro complexes, which typically exhibit $\nu_{as}(NO_2)$ and $\nu_s(NO_2)$ bands in the ranges 1470–1370 and 1340–1290 cm^{-1} respectively

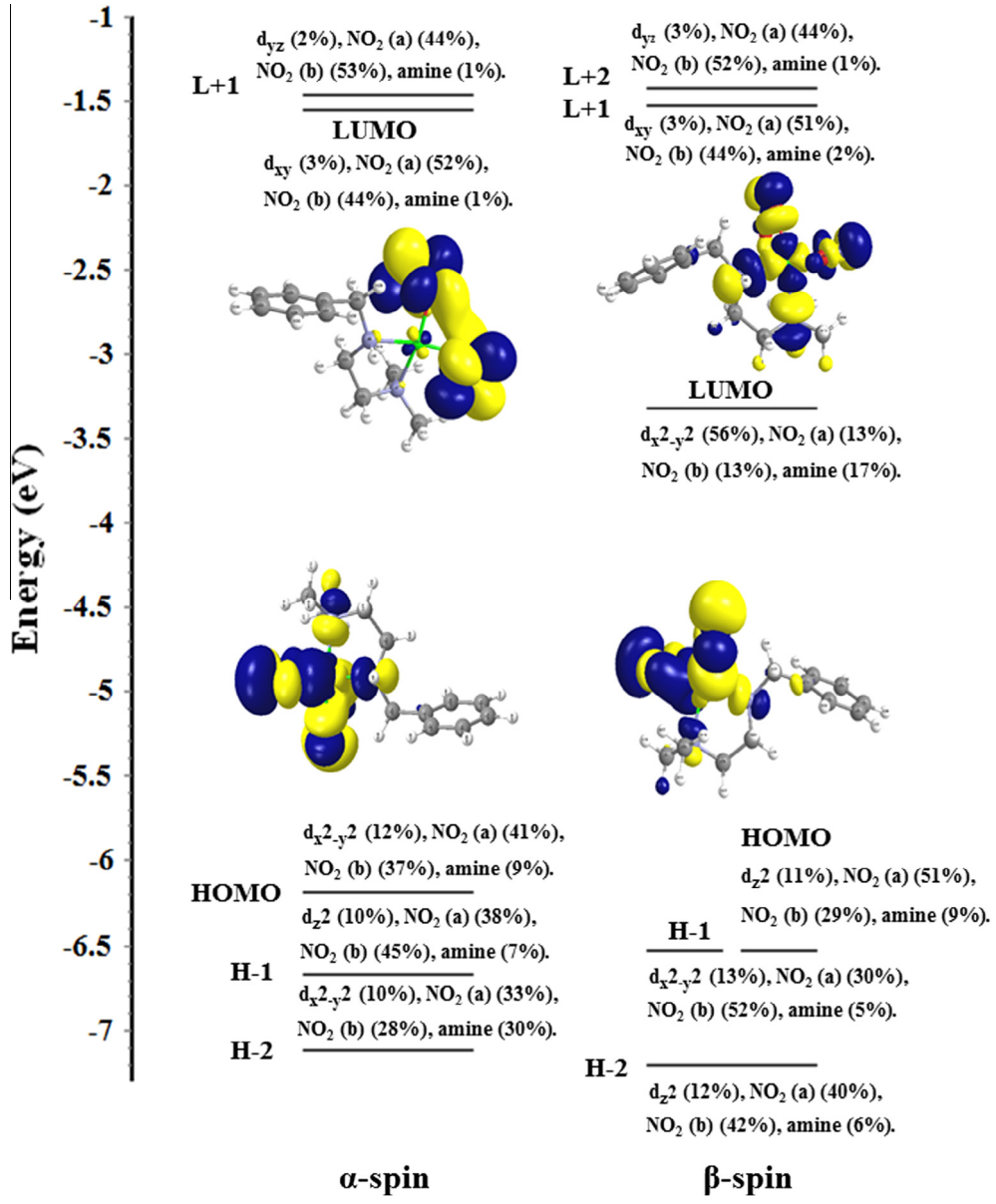

Fig. 7. The energy (eV), character and some contours of the unoccupied molecular orbitals of [Cu(L^{Me})(η^2-ONO)$_2$]. Positive values of the orbital contour are represented in yellow and negative values – in blue. (Color online.).

[46]. The most relevant feature in the chelating coordination of the η^2-ONO nitrite is the appearance of vibrational bands at 1365, 1160 and 870 cm^{-1}, corresponding to the $\nu_{as}(NO_2)$, $\nu_s(NO_2)$ and $\nu_\delta(NO_2)$ absorption bands, respectively [47]. The IR spectrum of **1** shows a strong band at 1350 cm^{-1} associated with $\nu_{as}(NO_2)$, two intense bands at 1170 and 1167 cm^{-1} related to $\nu_s(NO_2)$ and a medium peak at 849 cm^{-1} associated with $\nu_\delta(NO_2)$. These bands appear at 1347, 1197, 1171 and 843 cm^{-1} for compound **2** and 1393, 1271, 1217 and 830 cm^{-1} in compound **3** (Table S6 in the Supplementary information). The position of these vibrational bands and the separation between the ν_{as} and ν_s bands supports the asymmetric chelating coordination of the nitrite ion. It is noteworthy to mention that $\nu_s(NO_2)$ is split due to the anisobidentate nature of the nitrite group in the complexes. The highest splitting is observed in [Cu(L^{iso})(η^2-ONO)$_2$], where the steric hindrance around the copper center is substantial. These data are consistent with the observations noted in the X-ray crystallography section above. In fact, the N–O stretching frequencies vary almost linearly with the observed differences in N–O bond distances. That is, the longest N–O bond distance involves the O-atom most strongly bound to Cu(II), while the shortest N–O bond distance involves that O-atom bound only weakly to Cu(II).

The calculated vibrational spectra of all the complexes show good agreement with those of the experimental spectra, as illustrated in Fig. 6 (and also Table S6 and Figs. S4–S6 in the Supplementary information). Most of the calculated frequencies in the DFT method are harmonized with the experimental frequencies. The correlation diagrams are presented in Fig. 5, which describe the agreement between the calculated and experimental wavenumbers.

3.3.2. NBO analysis

Atomic charge analyses and natural electron configurations were performed to gain an insight into the source of the observed difference in the relative energies of the nitro (η^1-NO_2) and chelating nitrite (η^2-ONO) more quantitatively, and also to achieve a

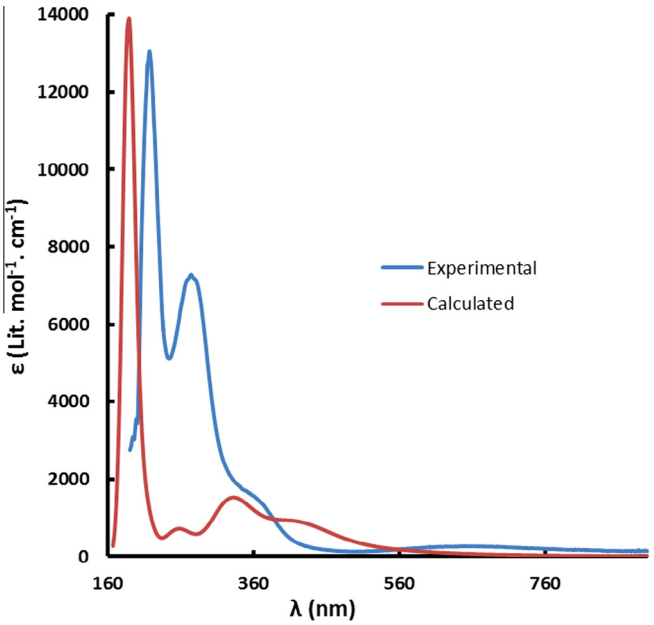

Fig. 8. The experimental (solid line) and calculated (dashed line) electronic absorption spectra of $[Cu(L^{Me})(\eta^2\text{-}ONO)_2]$ in methanol.

convenient basis to study charge transfer. Table S7 in the Supplementary information demonstrates the results of NPA calculations for the $L^RCu(\eta^1\text{-}NO_2)_2$ and $L^RCu(\eta^2\text{-}ONO)_2$ structures, with the two bare segments of $[L^RCu]$ and two nitrites as references. This result shows that the effective charges transferred from the chelating η^2-O,O nitrite ligands to the cationic complexes are −1.12, −1.12, −1.12 and −1.01 |e| in $[Cu(L^{Me})(NO_2)_2]$, $[Cu(L^{Et})(NO_2)_2]$, $[Cu(L^{iso})(NO_2)_2]$ and $[Cu(L^{tert\text{-}Bu})(NO_2)_2]$, respectively, whereas the effective charge transfers from the dinitro (η^1-NO_2) isomers are smaller, being −1.02, −1.02, −0.97 and −0.99 |e|, respectively. Furthermore, the charge delocalization on the NO_2 fragments in the nitro (η^1-NO_2) isomers is less than that of the chelating η^2-ONO isomers. As a result, the chelating η^2-ONO isomers are more stable than the nitro isomers in all cases, which is consistent with the experimental data in the solid state. The selected natural electron configurations for compounds **1–4** are shown in Table S7 in the Supplementary information. As indicated from the table, it can be concluded that the coordination of the Cu(II) ion by the O atoms is mainly on the 3*d*, 4*s* and 4*p* orbitals (the electron numbers of the 4*d* and 5*p* orbitals are so small they can be considered as negligible), while four O atoms bonding with the Cu(II) atom are all on the 2*s* and 2*p* orbitals (the electron number of 3*p* is insignificant).

3.3.3. Electronic structure and optical absorption spectra

The geometries of compounds **1–4** were optimized in the doublet state using the DFT method with the B3LYP/6-31G+ functional and the mixed basis set LANL2DZ/6-31G$^+$(*d*,*p*) in the gas phase. Schematic illustrations of the energy and character of selected frontier orbitals are shown in Fig. 7 and Figs. S7–S9 in the Supplementary information. An inspection of the DFT-calculated HOMOs of the complexes show that the β-spin HUMO and LUMO-1 in compounds **1–3** are very close in energy, thus can be considered as degenerate, being significantly of η^2-ONO ligand character (79%–83%) with small contributions from the d orbitals of copper(II) (11%–12%) and the diamine ligand (6%–9%), while the β-spin LUMOs are predominantly Cu d orbitals (d_{x2-y2} d_{xy}) (54%–55%) with some contribution from nitrite and diamine orbitals (16%–18%). Therefore, this can support electron donation of the η^2-ONO π electron to the copper $d\sigma$ orbital to form the primary σ bond, and this bond is further stabilized by back-donating from the copper $d\pi$ orbitals to the π^* anti-bonding orbitals of η^2-ONO moieties in the complexes.

TD-DFT analysis was performed with methanol as the solvent. The Polarizable Continuum model with Cosmo (the conductor-like screening model) (CPCM) was used [48] starting from the ground-state geometry optimization in solution without any symmetry constraints. The lowest 120 spin-allowed excitation states were taken into account for the calculations of the electronic absorption spectra of the complexes. TD-DFT calculations in solution provided absorption spectra for **1**–**3** in good agreement with the experimental results. For computational convenience, in the case of $[Cu(L^{tert\text{-}but})(\eta^2\text{-}ONO)_2]$, the methyl groups of the diamine ligand in the experimental $[Cu(L^{Me})(\eta^2\text{-}ONO)_2]$ complex were replaced by bulkier *tert*-butyl groups. It was separately checked that this substitution did not lead to appreciable changes in the electronic structure. Compounds **1**–**3** display two clear absorption bands along with a shoulder in the high energy region (UV region). Moreover, a weaker broad absorption band with a red shift in energy was also observed (Fig. 8 and S10-S12) in all complexes, which was assigned as a ligand field *d*–*d* transition. The TDDFT/PCM calculations demonstrated that the longest wavelength experimental absorptions at 662.0 nm for **1** and 651.0 nm for **2** and 706 nm for **3** originate from the transitions between some of the lowest β-spin HOMO orbitals and β-spin LUMO orbital. As can be observed from Fig. 8, S10 and S11, the LUMO orbital with β-spin is composed of mainly a *d* copper orbital, whereas the lowest β-spin HOMO orbitals are localized on the nitrite or diamine ligands, with admixtures of *d*Cu orbitals. Hence, the transitions assigned to these absorptions can be seen as mixed d → d (LF) and NO_2 → d (LMCT). The absorption bands at 274 and 217 nm for **1**, 282 and 219 nm for **2** and 258 and 227 nm for **3** involve a multitude of electronic transitions calculated in the 400–200 nm region, but the maximum contributions are from transitions of π(nitrite)/d → π^*/(nitrite)/*d* character. The calculated peaks correspond to charge transfer transitions that are comparative to the experimental results and their major contributions and character are summarized in Tables S8–S11 in the Supplementary information.

4. Conclusion

Structural and spectroscopic studies on copper(II)-dinitrito complexes using the ligands with different alkyl groups presented here allow for the determination of the properties of this system as a function of the applied steric hindrance. In the all complexes studied experimentally, the nitrite ions are bound in (η^2-ONO) bidentate mode to the copper(II) center. However there is an important difference among the complexes depending on whether there are sterically demanding alkyl substituents present in the diamine coligand or not. Using a less demanding ligand (dimethyl substituents), the nitrite binding mode is almost symmetric. However, the complex with the bulkier ligand shows an asymmetric binding of the nitrite ligand. Whereas this change of binding mode is nicely reflected by the vibrational properties of the complexes, the electronic absorption spectra are hardly affected. This is a very good example on how steric crowding around the copper center can influence the binding properties of the nitrite ligand. In this case, a change in the bulkiness of the coligand leads to an alteration of the properties of the metal site. The comparison of theoretical and experimental data shows a good correlation, confirming the reliability of the methods employed in this work and the theoretical results indicate that the density functional B3LYP method is able to provide satisfactory data. In this regard, the vibrational spectra of the (η^2-ONO)-coordinated nitrite complexes were reassigned. Moreover, the structure and vibrational spectrum of the

copper(II) complex of the *N*,*N*-di-tert-butyl,*N*′-benzyl-ethylenediamine ligand with a (η^2-ONO)-coordinated nitrite coligand were determined theoretically.

Acknowledgement

We are grateful for the financial support of the University of Mazandaran of the Islamic Republic of Iran.

Appendix A. Supplementary data

CCDC 1040208 and 1040214 contain the supplementary crystallographic data for [Cu(L^{Me}) (NO_2)$_2$] and [Cu(L^{Et})(NO_2)$_2$], respectively. These data can be obtained free of charge via http://www.ccdc.cam.ac.uk/conts/retrieving.html, or from the Cambridge Crystallographic Data Centre, 12 Union Road, Cambridge CB2 1EZ, UK; fax: (+44) 1223-336-033; or e-mail: deposit@ccdc.cam.ac.uk. Supplementary data associated with this article can be found, in the online version, at http://dx.doi.org/10.1016/j.poly.2015.01.044.

References

[1] G. Bombieri, G. Bruno, M. Cusumano, G. Gugliflmo, Acta Crystallogr. C 40 (1984) 409.
[2] J.A. Moser, R.A. Stockland Jr., G.K. Anderson, Polyhedron 19 (2000) 1329.
[3] J.R. Gispert, Coordination Chemistry, Wiley-VCH, Weinheim, 2008.
[4] J. Heinecke, P.C. Ford, Coord. Chem. Rev. 254 (2010) 235.
[5] M.A. DeLeo, P.C. Ford, Coord. Chem. Rev. 208 (2000) 47.
[6] D.M.L. Goodgame, M.A. Hitchman, Inorg. Chem. 3 (1964) 1389.
[7] N. Lehnert, U. Cornelissen, F. Neese, T. Ono, Y. Noguchi, K.-I. Okamoto, K. Fujisawa, Inorg. Chem. 46 (2007) 3916.
[8] W.B. Tolman, J. Biol. Inorg. Chem. 11 (2006) 261.
[9] I. Moura, J.J.G. Moura, Curr. Opin. Chem. Biol. 5 (2001) 168.
[10] I.M. Wasser, S. de Vries, P. Moenne-Loccoz, I. Schroder, K.D. Karlin, Chem. Rev. 102 (2002) 1201.
[11] B.A. Averill, Chem. Rev. 96 (1996) 2951.
[12] E.T. Adaman, J.W. Godden, S. Turley, J. Biol. Chem. 270 (1995) 27458.
[13] M.E.P. Murphy, S. Turley, E.T. Adman, J. Biol. Chem. 45 (1997) 28455.
[14] R.W. Strange, F.E. Dodd, Z.H.L. Abraham, J.G. Grossmann, T. Bruser, R.R. Eady, B.E. Smith, S.S. Hasnain, Nat. Struct. Biol. 2 (1995) 287.
[15] E.I. Tocheva, F.I. Rosell, A.G. Mauk, M.E.P. Murphy, Science 304 (2004) 867.
[16] N. Lehnert, U. Cornelissen, F. Neese, T. Ono, Y. Noguchi, K.I. Okamoto, K. Fujisawa, Inorg. Chem. 46 (2007) 3916.
[17] I.M. Wasser, S. de Vries, P. Moënne-Loccoz, I. Schröder, K.D. Karlin, Chem. Rev. 102 (2002) 1201.
[18] S. Suzuki, K. Kataoka, K. Yamaguchi, Acc. Chem. Res. 33 (2000) 728.
[19] W.B. Tolman, Inorg. Chem. 30 (1991) 4877.
[20] M. Calligaris, Coord. Chem. Rev. 248 (2004) 351.
[21] P. Coppens, I. Novozhilova, A. Kovalevsky, Chem. Rev. 102 (2002) 861.
[22] C.-S. Chen, H.-F. Dai, C.-H. Chen, W.-Y. Yeh, Inorg. Chim. Acta 376 (2011) 396.
[23] I.V. Novozhilova, P. Coppens, J. Lee, G.B. Richter-Addo, K.A. Bagley, J. Am. Chem. Soc. 128 (2006) 2093.
[24] S.E. Dominguez, P. Albores, F. Fagalde, Polyhedron 67 (2014) 471.
[25] H. Golchoubian, E. Rezaee, J. Mol. Struct. 929 (2009). 154-148.
[26] Bruker AXS Inc., SMART, Version 5.060 and SAINT, Version 6.02, Madison, Wisconsin, USA, 1999.
[27] M.C. Burla, R. Caliandro, M. Camalli, B. Carrozzini, G.L. Cascarano, L. De Caro, C. Giacovazzo, G. Polidori, R. Spagna, J. Appl. Crystallogr. 38 (2005) 381.
[28] G.M. Sheldrick, SHELXL97, Program for Crystal Structure Refinement, University of Göttingen, Germany, 1997.
[29] SHELXT LN, Version 5.10, Bruker Analytical X-ray Inc., Madison, WI, USA, 1998.
[30] GAUSSIAN 09, Revision A.02 M.J. Frisch, G.W. Trucks, H.B. Schlegel, G.E. Scuseria, M.A. Robb, J.R. Cheeseman, G. Scalmani, V. Barone, B. Mennucci, G.A. Petersson, H. Nakatsuji, M. Caricato, X. Li, H.P. Hratchian, A.F. Izmaylov, J. Bloino, G. Zheng, J.L. Sonnenberg, M. Hada, M. Ehara, K. Toyota, R. Fukuda, J. Hasegawa, M. Ishida, T. Nakajima, Y. Honda, O. Kitao, H. Nakai, T. Vreven, J.A. Montgomery Jr, J.E. Peralta, F. Ogliaro, M. Bearpark, J.J. Heyd, E. Brothers, K.N. Kudin, V.N. Staroverov, R. Kobayashi, J. Normand, K. Raghavachari, A. Rendell, J.C. Burant, S.S. Iyengar, J. Tomasi, M. Cossi, N. Rega, J.M. Millam, M. Klene, J.E. Knox, J.B. Cross, V. Bakken, C. Adamo, J. Jaramillo, R. Gomperts, R.E. Stratmann, O. Yazyev, A.J. Austin, R. Cammi, C. Pomelli, J.W. Ochterski, R.L. Martin, K. Morokuma, V.G. Zakrzewski, G.A. Voth, P. Salvador, J.J. Dannenberg, S. Dapprich, A.D. Daniels, O. Farkas, J.B. Foresman, J.V. Ortiz, J. Cioslowski, D.J. Fox, Gaussian Inc, Wallingford CT, 2009.
[31] R. Dennington, T. Keith, J. Millam, Semichem Inc., Shawnee Mission KS, GaussView, Version 5, 2009.
[32] C. Adamo, V. Barone, J. Chem. Phys. 108 (1998) 664.
[33] J.P. Perdew, Phys. Rev. B 33 (1986) 8822.
[34] A.D. Becke, J. Chem. Phys. 98 (1993) 5648.
[35] C. Lee, W. Yang, R.G. Parr, Phys. Rev. B 37 (1988) 785.
[36] M.J. Frisch, J.A. Pople, J.S. Binkley, J. Chem. Phys. 80 (1984) 3265.
[37] B. Machura, A. Świtlicka, M. Penkala, Polyhedron 45 (2012) 221.
[38] F. Neese, Coord. Chem. Rev. 253 (2009) 526.
[39] S. Ghosh, G.K. Chaitanya, K. Bhanuprakash, Md.K. Nazeeruddin, M. Grätzel, P.Y. Reddy, Inorg. Chem. 45 (2006) 7600.
[40] B. Machura, J.G. Małecki, A. Świtlicka, I. Nawrot, R. Kruszynski, Polyhedron 30 (2011) 864.
[41] A.E. Feed, F. Weinhold, J. Chem. Phys. 83 (1985) 1736.
[42] A.E. Feed, L.A. Curtiss, F. Weinhold, Chem. Rev. 88 (1988) 899.
[43] S. Youngme, N. Chaichit, C. Pakawatchai, S. Booncoon, Polyhedron 21 (2002) 1279.
[44] I.M. Procter, F.S. Stephans, J. Chem. Soc. A (1969) 1248.
[45] M.G.B. Drew, D. Rogers, Chem. Commun. (1965) 476.
[46] K. Nakamoto, Infrared and Raman Spectra of Inorganic and Coordination Compounds, fourth ed., Wiley, New York, 1986. p. 221.
[47] S. Youngme, S.I. Tonpho, K. Chinnakali, S. Chantrapromma, H.-K. Fun, Polyhedron 18 (1999) 851.
[48] M. Cossi, N. Rega, G. Scalmani, V. Barone, J. Comput. Chem. 24 (2003) 669.